Euro. Jnl of Applied Mathematics (2014), *vol.* 25, *pp.* 213–229.
doi:10.1017/S0956792513000429

Intricate dynamics caused by facilitation in competitive environments within polluted habitat patches

JULIÁN LÓPEZ-GÓMEZ[1], MARCELA MOLINA-MEYER[2] and ANDREA TELLINI[1]

[1] *Departamento de Matemática Aplicada, Universidad Complutense de Madrid, 28040 Madrid, Spain*
emails: Lopez_Gomez@mat.ucm.es
andrea.tellini@mat.ucm.es
[2] *Departamento de Matemáticas, Universidad Carlos III de Madrid, 28911 Leganés, Madrid, Spain*
email: mmolinam@math.uc3m.es

(*Received 2 April 2013; revised 2 December 2013; accepted 3 December 2013; first published online 7 January 2014*)

This paper analyses a canonical class of one-dimensional superlinear indefinite boundary value problems of great interest in population dynamics under non-homogeneous boundary conditions; the main bifurcation parameter in our analysis is the amplitude of the superlinear term. Essentially, it continues the analysis of López-Gómez *et al.* (López-Gómez, J., Tellini, A. & Zanolin, F. (2014) High multiplicity and complexity of the bifurcation diagrams of large solutions for a class of superlinear indefinite problems. *Comm. Pure Appl. Anal.* **13**(1), 1–73) with empty overlapping, by computing the bifurcation diagrams of positive steady states of the model and by proving analytically a number of significant features, which have been observed from the numerical experiments carried out here. The numerics of this paper, besides being very challenging from the mathematical point of view, are imperative from the point of view of population dynamics, in order to ascertain the dimensions of the unstable manifolds of the multiple equilibria of the problem, which measure their degree of instability. From that point of view, our results establish that under facilitative effects in competitive media, the harsher the environmental conditions, the richer the dynamics of the species, in the sense discussed in Section 1.

Key words: Facilitation in polluted patches; Bifurcation diagrams; Superlinear indefinite problems; Unstable manifolds; Degree of instability; Uniqueness of local attractor

1 Introduction

This paper deals with the existence, multiplicity and stability of the positive equilibria of

$$\begin{cases} \partial_t u - \partial_{xx} u = \lambda u + a_b(x) u^p & x \in (0,1), \quad t > 0, \\ u(0,t) = u(1,t) = M, & t > 0, \\ u(x,0) = u_0(x), & x \in (0,1), \end{cases} \tag{1.1}$$

where $u_0 > 0$ is a given positive function, $M > 0$, $p > 1$, $\lambda < 0$ is regarded as a real parameter and $a_b(x)$ is the symmetric piece-wise constant function defined by

$$a_b(x) = \begin{cases} -c \text{ if } x \in [0,\alpha) \cup (1-\alpha, 1] \\ b \quad \text{if } x \in [\alpha, 1-\alpha] \end{cases}$$

for some $\alpha \in (0, 0.5)$, $b \geqslant 0$ and $c > 0$; the steady states of (1.1) are the positive solutions of the one-dimensional boundary value problem

$$\begin{cases} -u'' = \lambda u + a_b(x) u^p \quad \text{in } (0,1), \\ u(0) = u(1) = M. \end{cases} \tag{1.2}$$

Problem (1.1) is of sublinear degenerate type if $b = 0$, while it is a superlinear indefinite problem if $b > 0$, as in this case a_b changes sign in $[0,1]$. These problems have attracted a huge attention during the last two decades, as it becomes apparent by simply having a look at [1, 5–7, 18, 21, 22, 27–29, 39] and references therein.

In population dynamics, (1.1) models the evolution of a single species in a harsh (one-dimensional) inhabiting region, the interval $(0,1)$, which is surrounded by territories where the population density equals M. In these models $u(x,t)$ stands for the density of the species at the location $x \in (0,1)$ and at time $t > 0$, $\lambda < 0$ measures the neat death rate of the species in $(0,1)$ and $u_0 > 0$ is the initial population density. In nature, λ is negative, for example, when pesticides are used in high concentrations, or a certain patch of the environment is polluted by introducing chemicals, waste products or poisonous substances.

When $b = 0$, as $a_0 = 0$ in $(\alpha, 1-\alpha)$, the species u grows in that patch according to Malthus' law and, in particular, the resources are unlimited therein, whereas the evolution of u is governed by the logistic law, with exponent p, in $(0,\alpha) \cup (1-\alpha, 1)$. In such a case, according to [30], (1.2) admits a unique positive solution, denoted by $\theta_{[\lambda,M]}$, which is a global attractor for (1.1). Naturally, $\theta_{[\lambda,M]} < M$ in the inhabiting region because $\lambda < 0$, and hence $u'' > 0$. Essentially, through the edges of the polluted area there is a continuous flow of individuals who die in the interior at the rate $\lambda < 0$ by the action of a contaminant. The continuous flow of individuals through the boundary of the poisoned region can maintain the population at $\theta_{[\lambda,M]}$ level as time grows. Basically, the same situation occurs if $\lambda > 0$, but the length of $(\alpha, 1-\alpha)$ is sufficiently small so that $\lambda < [\pi/(1-2\alpha)]^2$. Surprisingly, when the birth rate of the species, measured by λ, crosses the threshold $[\pi/(1-2\alpha)]^2$, the population remains bounded in $(0,\alpha) \cup (1-\alpha, 1)$, much like in the classical logistic model, while it grows approximating infinity in $(\alpha, 1-\alpha)$, which is the region where the evolution of u is governed by Malthus' law.

The main goal of this paper is to analyse how the dynamics of (1.1) changes as the parameter $b > 0$ varies, perturbing from 0, when $\lambda < 0$. In population dynamics, $b > 0$ measures the interspecific facilitative effects of the species u in the patch $(\alpha, 1-\alpha)$. In these generalized logistic prototypes, the individuals of the species u compete for the natural resources in the region where $a_b < 0$, while they cooperate in the patches where $a_b > 0$.

Although there are extensive reviews about the experimental evidence of interspecific competition (see, e.g. [14, 42]) and positive interactions are well documented among organisms from different kingdoms, as they can make significant contributions to each other's needs without sharing the same resources (see, e.g. [24, 41, 43]), finding positive interactions among similar organisms seems to be a huge task in empirical studies, since they do not arise alone but in combination with competition. However, according to the abiotic stress hypothesis of [8], the importance of positive interactions in plant communities increases with abiotic stress or consumer pressure. Several empirical studies support the validity of the abiotic stress hypothesis and, actually, a substantial number among documented positive interactions in plant communities have been isolated in harsh environmental conditions (see, e.g. [12,40]). Consequently, (1.1) seems to be a rather reasonable mathematical model for studying the effects of combined facilitation and competition in polluted habitat patches.

By some classical results in elliptic regularity theory (see, e.g. [19]), any weak solution u of (1.2) must satisfy $u \in \mathscr{C}^\infty[0,\alpha) \cap \mathscr{C}^\infty[\alpha, 1-\alpha] \cap \mathscr{C}^\infty(1-\alpha, 1] \cap \mathscr{C}^1[0,1]$. Moreover, thanks to the maximum principle (see [32]), any non-negative solution of (1.2) must satisfy $u(x) > 0$ for all $x \in [0,1]$. These are the solutions considered in this paper, even if not said explicitly.

Problem (1.2) with a piece-wise constant a_b goes back to [38], where it was shown how the qualitative complexity of the global bifurcation diagrams of (1.2), using b as a main continuation parameter, increases dramatically as the secondary parameter $-\lambda > 0$ grows. From the perspective of population dynamics, it is imperative to design efficient numerical algorithms to compute the steady states of (1.1), as well as the dimensions of their respective unstable manifolds, which cannot be determined from the existing analytical tools. This is the first task that we have accomplished in this paper, in Section 2, through some extremely sophisticated, local and global path-following numerical solvers, which are not available in any commercial package, such as AUTO [16, p. 18], where the following is admitted: *Note that, given the non-adaptive spatial discretization, the computational procedure here is not appropriate for PDEs with solutions that rapidly vary in space, and care must be taken to recognize spurious solutions and bifurcations*. This is just one of the main problems that we found in our numerical experiments in Section 2, as the number of critical points of the solutions increases according to the dimensions of unstable manifolds, and the turning and bifurcation points are extremely close. As evidenced by the numerics, the following new findings become apparent:

- For every $\lambda < 0$, there is $b_c = b_c(\lambda) > 0$ such that the interval $(-\infty, b_c(\lambda)]$ provides us with the set of b's for which (1.2) admits a positive solution.
- $\lim_{\lambda \downarrow -\infty} b_c(\lambda) = +\infty$.
- The unique stable positive steady state of (1.1) is the minimal one, although (1.2) can admit an arbitrarily large number of solutions.

Actually, these are the main new findings of this paper, which will be proven in Sections 3 and 4. Although in this paper we often invoke some previous results going back to [4,30,38], the overlapping of our new results here with those of these three cited works is absolutely empty.

According to [38], it is already known that, for any integer $n \geqslant 0$, (1.2) possesses solutions with n strict critical points in the interval $(\alpha, 1-\alpha)$ if $-\lambda > 0$ is sufficiently large for certain ranges of b. Moreover, these solutions must be asymmetric if $n \geqslant 2$ is even in spite of the symmetry of the problem. The solution with 0 strict critical points, referred to as the *trivial solution* of (1.2), will play an important role in explaining and understanding the complexity of the global bifurcation diagrams of (1.2), as it behaves like an *organising centre* in singularity theory (see, e.g. [20]). It can be constructed as follows. Let $u_M(x)$ denote the unique solution of

$$\begin{cases} -u'' = \lambda u - cu^p & \text{in } (0,\alpha) \\ u(0) = M, \quad u'(\alpha) = 0 \end{cases},$$

and set $m_0 := u_M(\alpha)$. Then the constant function m_0 solves $-u'' = \lambda u + bu^p$ if and only if $b = b^*$, where $b^* := -\lambda/m_0^{p-1}$, and for such value of b the trivial solution u^* is defined through

$$u^*(x) = \begin{cases} u_M(x), & x \in [0,\alpha), \\ m_0, & x \in [\alpha, 1-\alpha], \\ u_M(1-x), & x \in (1-\alpha, 1], \end{cases} \tag{1.3}$$

which is symmetric around $x = 0.5$.

Basically, as illustrated by the left plot of Figure 1, for $\lambda < 0$, $\lambda \sim 0$, the global structure of the positive solutions of (1.2) consists of a *primary curve* establishing a homotopy between the unique solution of

$$\begin{cases} -u'' = \lambda u + a_0(x)u^p & \text{in } (0,1), \\ u(0) = u(1) = M, \end{cases} \tag{1.4}$$

and the *metasolution* (large solution prolonged by infinity)

$$m(x) := \begin{cases} u_\infty(x), & x \in [0,\alpha) \\ \infty, & x \in [\alpha, 1-\alpha] \\ u_\infty(1-x), & x \in (1-\alpha, 1] \end{cases},$$

where u_∞ stands for the unique solution of the singular problem

$$\begin{cases} -u'' = \lambda u - cu^p & \text{in } [0,\alpha) \\ u(0) = M, \quad u(\alpha) = \infty \end{cases}. \tag{1.5}$$

Then, as $-\lambda > 0$ increases, a piece of the primary curve rotates counterclockwise around the trivial solution u^* and almost after every half rotation an additional closed loop emanates from it. The loop consists of solutions of asymmetric type and it persists for all further values of $-\lambda$ (see the series of Figures 1–3). Indeed, thanks to [38], the number of turning points of the primary curve, as well as the number of bifurcation points along it, is unbounded as $\lambda \downarrow -\infty$. This explains why the numerics of (1.2) carried out in this paper is a mathematical challenge.

An astonishing phenomenon evidenced by our numerics in Section 2 is that the larger the value of $-\lambda$, the larger the range of values of the main parameter b for which (1.2) possesses some positive solution, and simultaneously smaller the positive solutions of (1.2) at α. This feature entails that the turning points of the primary curve are extremely closed, which makes the implementation of the numerical computations of this paper a very hard task. By simply having a glance at Figure 3, which represents the global bifurcation diagram of (1.2) for $\lambda = -2000$, the reader will easily realize what we mean. Although

$b_c = 1.2463985 \times 10^7$, most of the positive solutions in the diagram satisfy $u(\alpha) \sim 10^{-4}$, and, in addition, the first loop bifurcates from the primary branch at $b = 1.2463984 \times 10^7$, which is extremely close to b_c. Consequently, even looking so simple, the prototype model (1.2) generates highly intricate global bifurcation diagrams whose numerical computation is extremely challenging not only because of the complexity of the structure of the diagrams themselves but also by the scales of the parameters at which the phenomenologies of practical interest arise.

The organisation of this paper is as follows. Section 2 shows the numerical results, Section 3 establishes the existence of $b_c(\lambda)$ and shows that $\lim_{\lambda \downarrow -\infty} b_c(\lambda) = \infty$ and Section 4 proves that the minimal positive solution of (1.2) is the unique (locally) stable positive steady state of (1.1).

From the point of view of applications in population dynamics, our numerical experiments show that, under facilitative effects in competitive media, the harsher the environmental conditions, the richer the dynamics of the species. For example, for $\lambda = -2,000$, there is a range of values of b around $b^* = 0.7007 \times 10^7$ where (1.2) exhibits 12 positive solutions, say θ_j, $0 \leqslant j \leqslant 11$ (see Figure 3). Subsequently, for any $0 \leqslant j \leqslant 11$, we will denote by W_j^u (resp. W_j^s) the unstable (resp. stable) manifold of θ_j. According to Theorem 4.1, the minimal positive solution, say θ_0, is the unique local attractor of (1.1). Local attractor means that the unique solution of (1.1), denoted by $u(t;u_0)$, satisfies

$$\lim_{t\uparrow\infty} u(t;u_0) = \theta_0, \qquad \text{provided } \ u_0 \ \text{ is sufficiently close to } \ \theta_0,$$

i.e $W_0^u = \text{span}[0]$. Naturally, if u_0 stays far away from θ_0, $u(t;u_0)$ might approximate any of the remaining equilibria θ_j's, or it might oscillate among several of them for a sufficiently long time, or it might even approximate some metasolution. According to our numerical experiments in Section 2, the positive solutions of (1.2) at $\lambda = -2,000$ can be labelled so that

$$\dim W_j^u = \dim W_{11-j}^u = j, \quad 1 \leqslant j \leqslant 5, \qquad \dim W_{11}^u = 6.$$

It is well known that W_j^s is a local infinite-dimensional (nonlinear) sub-manifold of $\mathscr{C}[0,1]$ with

$$\text{codim}\, W_j^s = \dim W_j^u,$$

for all $0 \leqslant j \leqslant 11$. Moreover,

$$\lim_{t\uparrow\infty} u(t;u_0) = \theta_j \qquad \text{if } \ u_0 \in W_j^s, \qquad 0 \leqslant j \leqslant 11.$$

Consequently, each of the positive equilibria can be approximated by the solutions of (1.1) by choosing u_0 sufficiently close to θ_j on W_j^s, although if $u_0 \in W_j^u$, the solution will separate away from θ_j as time passes by. Ascertaining the behaviour of $u(t;u_0)$ in such cases is an extremely challenging open problem. These examples can be constructed for all θ_j, $1 \leqslant j \leqslant 11$, except for θ_0, since it is a local attractor. Precisely, the dimensions of the (local nonlinear) unstable manifold W_j^u measure the degree of instability of the corresponding θ_j.

The fact that the number of steady states of (1.1) grows arbitrarily as the degree of inhabitability of the environment blows up as an effect of interspecific facilitative effects.

This has been observed for the first time in this paper in the context of spatial ecology, and it might be a relevant feature in the theory of ecosystems.

2 A series of significant global bifurcation diagrams

Throughout this section we will fix $\alpha = 0.3$, $p = 2$, $M = 100$ and $c = 1$, whereas b and λ will be regarded as the primary and secondary parameters of the problem, respectively. Since the value of c is substantially smaller than M, the associated solutions of (1.2) can though be of approximations to the *large solutions* of the associated equation

$$-u'' = \lambda u + a_b(x)u^p.$$

A large solution means a classical solution with $u(0) = u(1) = \infty$ (see [30, 38]). Precisely, we will give to the parameter λ a series of significant values ranging in the interval $(-\infty, 0]$ and, for each of these values, b will be regarded as the main bifurcation parameter to compute the corresponding global bifurcation diagrams of (1.2). Our main goal is to show their complexity as $-\lambda > 0$ increases and to get some quantitative properties such as the dimensions of unstable manifolds of all positive solutions along them.

To discretize (1.2) we have used a pseudo-spectral method combining a trigonometric spectral method with collocation at equidistant points, as in most of our previous numerical works in [21, 23, 31, 33–36]. The spectral method uses trigonometric modes. This gives high accuracy at a very low computational cost (see, e.g. [13]). For general Galerkin approximations, the local convergence of paths at regular, turning and simple bifurcation points was proven in [9–11, 31, 37]. In all these situations, the local topological structures of the solution curves for the continuous and discrete models are equivalent. The global continuation solvers used to compute the solution curves, and the dimensions of the unstable manifolds of all the solutions along them have been built by ourselves from the theory on continuation methods of [2, 15, 17, 25, 26, 31].

The complexity of the bifurcation diagrams, as well as their quantitative features, required an extremely careful control of all the steps in subroutines. In the implementation of the available continuation methods, we found, essentially, two main difficulties. Namely, one must be extremely careful in choosing the shot direction to compute the bifurcated closed loops from the primary curve, and, in addition, one should adopt an appropriate re-scaling procedure to compute automatically all turning points along the primary curve as they are extremely closed. As a result, the available algorithms in the specialized literature do not work for sufficiently large $-\lambda > 0$; in particular, the standard bifurcation package AUTO cannot be used in our context.

The left picture in Figure 1 shows the plot of the bifurcation diagram of (1.2) for $\lambda = -5$. As in all subsequent bifurcation diagrams, we are representing the value of b in the horizontal axis versus the value of $u(\alpha)$ in the vertical one.

The bifurcation diagram consists of a single *primary curve* emanating from the unique positive solution of (1.4) at $b = 0$, whose existence and uniqueness was established in [30], and it continues towards the right to reach a critical value, $b = b_c$, where it goes backwards, exhibiting a subcritical turning point. Once it passed the turning point, the solutions on the upper half-branch can be continued for every $0 < b < b_c$ and as $b \downarrow 0$, they blow up in

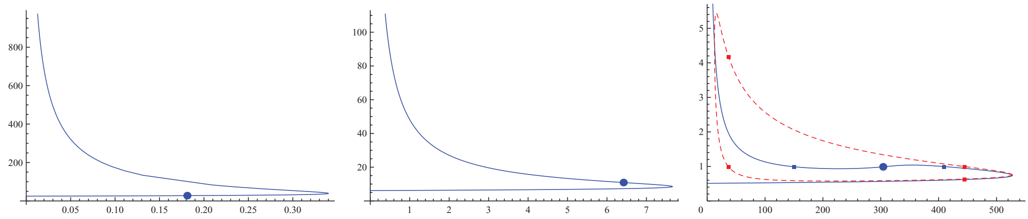

FIGURE 1. (Colour online) Bifurcation diagrams for $\lambda = -5$ (left), $\lambda = -70$ (centre) and $\lambda = -300$ (right). The thick points mark the position of u^* (see (1.3)). Small squares indicate changes in the number of critical points of the solution.

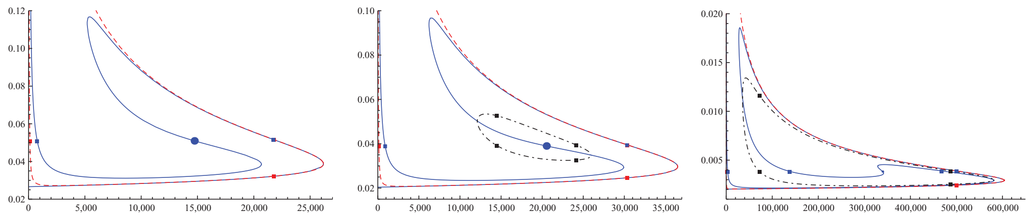

FIGURE 2. (Colour online) Global bifurcation diagram for $\lambda = -750$ (left), $\lambda = -800$ (centre) and $\lambda = -1300$ (right).

$[\alpha, 1-\alpha]$, while in $[0, \alpha)$ they approximate the unique solution u_∞ of the singular problem (1.5). Consequently, for every $b \in (0, b_c)$, (1.2) admits at least two solutions. The solutions along the lower half-branch are linearly asymptotically stable (local attractors), while those on the upper half-branch are unstable with one-dimensional unstable manifold. The centre plot in Figure 1 shows the bifurcation diagram for $\lambda = -70$. Now, as in all subsequent diagrams, u^* appears on the branch of linearly unstable solutions. The right diagram in Figure 1 has been computed for $\lambda = -300$ and exhibits a secondary loop bifurcated as a consequence of a *symmetry breaking* from the principal curve. The bifurcation points of the loop are of pitchfork type. As λ decreased from -70, there was the first value for which the loop appeared. Then the loop persisted for all smaller values of λ. The solutions on the loop are asymmetric, and for fixed b the one on its upper branch is the symmetrization of the one on the lower branch.

As λ decreased from $\lambda = -300$ to reach the value, $\lambda = -750$, whose associated global bifurcation diagram has been plotted in the first diagram in Figure 2, the primary branch rotated counterclockwise around u^*, originating two additional turning points along it: one of these turning points is supercritical and the other is subcritical. In this picture, as in all the subsequent ones, by the scale chosen in the plots, a piece of the first bifurcated loop could not be plotted.

Further, the second loop of asymmetric solutions emerged from the primary branch, following the same patterns as the first one. The central plot in Figure 2 shows it for $\lambda = -800$, while the right one shows the bifurcation diagram for $\lambda = -1,300$, where an additional rotation of the primary branch has occurred. This alternation between rotations of the principal branch around the trivial solution and secondary bifurcations of loops of asymmetric solutions is maintained as λ decreases, as it can be inferred from the

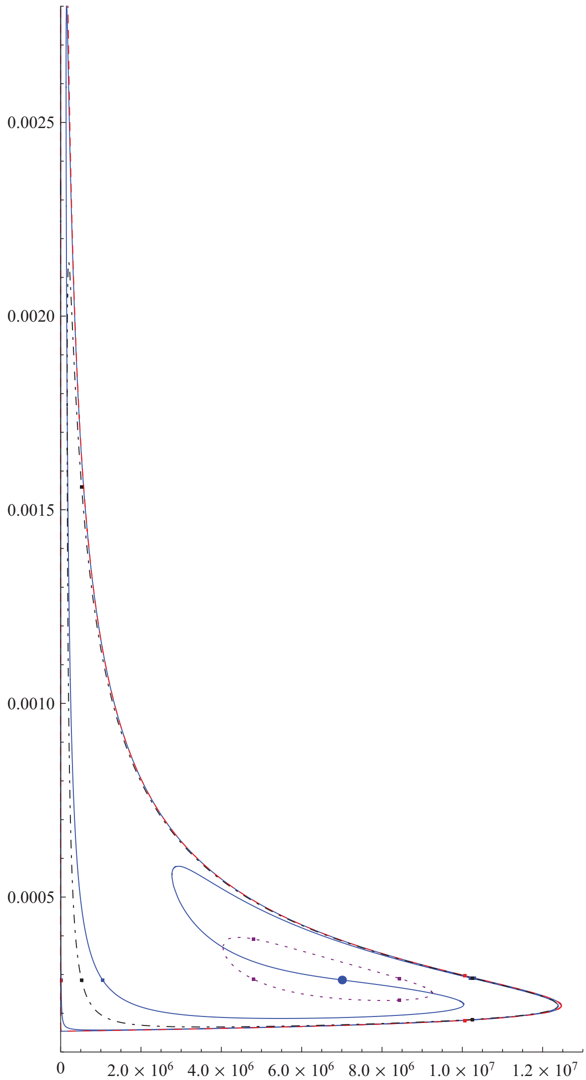

FIGURE 3. (Colour online) Global bifurcation diagram for $\lambda = -2,000$.

bifurcation diagram in Figure 3, computed for $\lambda = -2,000$. Therefore, there are ranges of the parameter b for which number of solutions of (1.2) grows arbitrarily as $\lambda \downarrow -\infty$.

The solutions on the primary branch are symmetric about 0.5, with a single strict critical point in $(\alpha, 1-\alpha)$ until b reaches a certain critical value, the one marked with a small square in the diagrams, where the number of critical points increases by two. This pattern is maintained until u^* is reached, and afterwards the number of critical points decreases by two at every small square, to become one again. In most of the cases, along the nth loop, the (asymmetric) solutions have $2n-1$ strict critical points near the bifurcation points and $2n$ critical points in the central parts of the loop. An absolutely new and rather remarkable feature, which could not be observed in [38], is the fact that the dimensions of unstable manifolds of all the solutions along the primary curve increase by one, starting with 0 (at $b = 0$), each time that a bifurcation, or a turning point, is crossed, until the interior of the last emanated loop is reached. Then these dimensions decrease, according to the same rule, until they became one-dimensional again. In particular, although the model can have an arbitrarily large number of steady states, the numerics suggest that the minimal one is a unique linearly stable steady state, i.e. a unique local attractor – an absolutely new feature that will be proven analytically in Section 4.

3 Some sharp existence results

By simply having a glance at the bifurcation diagrams of Figures 1–3, it is easily realized that the maximal value of b for which the problem admits a positive steady state should approximate ∞ as $\lambda \downarrow -\infty$. The following result establishes it rigourously.

Theorem 3.1 *For every $\lambda < 0$ there exists $b_c = b_c(\lambda) > 0$ such that* (1.2) *has a positive solution for each $b \in [0, b_c(\lambda))$ and it does not admit any positive solution if $b > b_c(\lambda)$. Moreover,* (1.2) *has a minimal positive solution if it admits some, which is linearly stable. Furthermore,*

$$\lim_{\lambda \downarrow -\infty} b_c(\lambda) = \infty. \tag{3.1}$$

Proof Fix $\lambda < 0$ and consider the associated sublinear problem (1.4). As a consequence from [30, Th. 3.5], (1.4) possesses a unique positive solution, which is linearly asymptotically stable. Thus, according to the implicit function theorem, there exists $\delta > 0$ such that (1.2) admits a positive solution for each $b \in [0, \delta)$. On the other hand, based on [29, Th. 4.1(b)], it becomes apparent that (1.2) cannot admit any positive solution for sufficiently large $b > 0$, because the positive solutions of (1.1) blow up in a finite time. Moreover, using the method of sub- and super-solutions, it is easy to see that (1.2) possesses a positive solution for all $b \in [0, b_0]$ if it admits a positive solution for $b = b_0$. Therefore, the existence of $b_c(\lambda) > 0$ satisfying the requirements of the statement of the theorem holds. Next, we will show the existence and the local linearized stability of the minimal positive solution of (1.2). Suppose (b, u) is a solution of (1.2) with $b > 0$. As $(0, u)$ is an ordered sub-supersolution pair, the existence of a (unique) minimal solution $u_{\min}$ in the ordered interval $[0, u]$ follows from [4, Th. 6.1]. The linear stability of $u_{\min}$ can be obtained by contradiction, as in [4, Th. 7.3]. Indeed, suppose that $\sigma := \sigma[\mathfrak{L}_{(b,u_{\min})}] < 0$, where, for any given positive solution (b, u) of (1.2),

$$\mathfrak{L}_{(b,u)} := -\frac{d^2}{dx^2} - \lambda - a_b p u^{p-1}$$

and $\sigma[\mathfrak{L}_{(b,u)}]$ stands for the principal eigenvalue of $\mathfrak{L}_{(b,u)}$ in $(0, 1)$ under homogeneous Dirichlet boundary conditions. Let $\phi > 0$ be an eigenfunction associated with σ. We claim that $\bar{u} := u_{\min} - \epsilon\phi > 0$ is a strict supersolution to (1.2) for sufficiently small $\epsilon > 0$. Indeed, according to the definition of $u_{\min}$ and ϕ, we find that

$$-\bar{u}'' = \lambda\bar{u} + a_b \left(u_{\min}^p - \epsilon p \phi u_{\min}^{p-1}\right) - \epsilon\sigma\phi \quad \text{in } (0, 1). \tag{3.2}$$

https://doi.org/10.1017/S0956792513000429 Published online by Cambridge University Press

Now, setting $f(\epsilon) := (u_{\min} - \epsilon\phi)^p$, the Taylor formula for $\epsilon \sim 0$ yields

$$\bar{u}^p = f(\epsilon) = f(0) + \epsilon f'(0) + o(\epsilon) = u_{\min}^p - \epsilon p \phi u_{\min}^{p-1} + o(\epsilon)$$

and hence, since $\sigma < 0$, it becomes apparent from (3.2) that

$$-\bar{u}'' = \lambda\bar{u} + a_b\bar{u}^p - \epsilon\sigma\phi + o(\epsilon) > \lambda\bar{u} + a_b\bar{u}^p \quad \text{in } (0,1)$$

for sufficiently small $\epsilon > 0$. Moreover, $\bar{u}(0) = \bar{u}(1) = M$, by construction. As $\bar{u} > 0$ for sufficiently small $\epsilon > 0$ and zero is a sub-solution of (1.2), once again from [4, Th. 6.1], we find that (1.2) possesses a minimal positive solution in $[0, u_{\min} - \epsilon\phi]$. Naturally, this contradicts the minimality of $u_{\min}$ and hence it shows that $\sigma \geqslant 0$. This concludes the proof of the existence and linear stability of the minimal positive solution of (1.2).

To prove (3.1) we will use the next lemma.

Lemma 1 *Suppose $\lambda < 0$, $L > 0$, and $M_1, M_2 \in (0, \infty]$. Then the problem*

$$\begin{cases} -u'' = \lambda u - cu^p & \text{in } (0, L), \\ u(0) = M_1, \quad u(L) = M_2, \end{cases} \tag{3.3}$$

has a unique positive solution; denoted by $u = u_\lambda$. Moreover,

$$\lim_{\lambda \downarrow -\infty} u_\lambda = 0 \qquad \text{uniformly on compact subsets of} \quad (0, L). \tag{3.4}$$

Proof The existence and the uniqueness of u_λ are easy consequences from [30, Th. 3.5]. Moreover, it follows from the maximum principle that $0 < u_\lambda < u_\mu < u_0$ if $\lambda < \mu < 0$, and hence $\lim_{\lambda\downarrow-\infty} u_\lambda < u_0$ is well defined. Let $0 < x_1 < x_2 < L$ and consider the function

$$\varphi(x) := \sin\left(\frac{\pi(x - x_1)}{x_2 - x_1}\right), \qquad x \in [x_1, x_2].$$

Multiplying the differential equation of (3.3) by φ and integrating by parts in (x_1, x_2) yields

$$\begin{aligned} \lambda \int_{x_1}^{x_2} u_\lambda\varphi - c\int_{x_1}^{x_2} u_\lambda^p\varphi &= -\int_{x_1}^{x_2} u_\lambda''\varphi = -\left[u_\lambda'\varphi\right]_{x_1}^{x_2} + \int_{x_1}^{x_2} u_\lambda'\varphi' \\ &= \int_{x_1}^{x_2} \left[(u_\lambda\varphi')' - u_\lambda\varphi''\right] \\ &= u_\lambda(x_2)\varphi'(x_2) - u_\lambda(x_1)\varphi'(x_1) + \left(\frac{\pi}{x_2 - x_1}\right)^2 \int_{x_1}^{x_2} u_\lambda\varphi \end{aligned}$$

and hence,

$$\begin{aligned} \left[\lambda - \left(\frac{\pi}{x_2 - x_1}\right)^2\right] \int_{x_1}^{x_2} u_\lambda\varphi - c\int_{x_1}^{x_2} u_\lambda^p\varphi &= u_\lambda(x_2)\varphi'(x_2) - u_\lambda(x_1)\varphi'(x_1) \\ &> u_0(x_2)\varphi'(x_2) - u_0(x_1)\varphi'(x_1), \end{aligned}$$

https://doi.org/10.1017/S0956792513000429 Published online by Cambridge University Press

because $\varphi'(x_2) < 0 < \varphi'(x_1)$. Therefore,

$$\left[\lambda - \left(\frac{\pi}{x_2 - x_1}\right)^2\right] \int_{x_1}^{x_2} u_\lambda \varphi > u_0(x_2)\varphi'(x_2) - u_0(x_1)\varphi'(x_1)$$

and, consequently, letting $\lambda \downarrow -\infty$ in this inequality, (3.4) holds. □

We have all the ingredients to complete the proof of (3.1). By [38, Th. 3.3], we have that

$$b^*(\lambda) := -\lambda/m_0(\lambda)^{\frac{1}{p-1}} \leqslant b_c(\lambda),$$

because (1.2) admits a positive solution for $b = b^*(\lambda)$; remember that we are denoting $m_0(\lambda) := u(\alpha)$, where u a unique solution of

$$\begin{cases} -u'' = \lambda u - cu^p \quad \text{in } (0, \alpha), \\ u(0) = M, \quad u'(\alpha) = 0. \end{cases}$$

By Lemma 1 applied with $L = 2\alpha$ and $M_1 = M_2 = M$, we find that

$$\lim_{\lambda \downarrow -\infty} m_0(\lambda) = 0.$$

Consequently,

$$\lim_{\lambda \downarrow -\infty} b^*(\lambda) = \infty \leqslant \liminf_{\lambda \downarrow -\infty} b_c(\lambda).$$

The proof is complete. □

4 Uniqueness of the stable solution

The main result of this section shows that (1.1) possesses a unique linearly stable positive steady state for all $b \geqslant 0$ for which (1.2) admits a positive solution. It can be stated as follows.

Theorem 4.1 *Suppose* (1.2) *admits a positive solution for $b = b_0 > 0$ and let (b_0, u_0) denote the minimal one. Then, (b_0, u_0) is the unique linearly stable positive solution of* (1.1).

The proof of this theorem follows after a series of preliminary technical results.

Proposition 1 *Let (b_0, u_0) be a linearly asymptotically stable positive solution of* (1.2). *Then there exist $\epsilon > 0$ and a differentiable map $u : (b_0-\epsilon, b_0+\epsilon) \to \mathscr{C}^1(\bar{\Omega})$ such that $u(b_0) = u_0$ and $(b, u(b))$ is a linearly asymptotically stable positive solution of* (1.2) *for all $b \in (b_0-\epsilon, b_0+\epsilon)$. Moreover, the map $(b_0 - \epsilon, b_0 + \epsilon) \to \mathscr{C}(\bar{\Omega})$, $b \mapsto u(b)$ is increasing and there exists a neighbourhood $\mathscr{U}$ of (b_0, u_0) in $\mathbb{R} \times \mathscr{C}^1(\bar{\Omega})$ such that $\mathscr{P}_b(\mathscr{U}) \subset (b_0 - \epsilon, b_0 + \epsilon)$ and $(b, u) = (b, u(b))$ if $(b, u) \in \mathscr{U}$ is a solution of* (1.2)*; $\mathscr{P}_b$ stands for the projection operator on b.*

Proof The solutions of (1.2) are the zeros of the operator $\mathfrak{F} : \mathbb{R} \times \mathscr{C}_0^1(\bar{\Omega}) \to \mathscr{C}_0^1(\bar{\Omega})$ defined by

$$\mathfrak{F}(b, v) := v - (-\Delta)^{-1}\left[\lambda(v + M) + a_b(v + M)^p\right]. \tag{4.1}$$

https://doi.org/10.1017/S0956792513000429 Published online by Cambridge University Press

As (b_0, u_0) solves (1.2), setting $v_0 := u_0 - M$ we have that $\mathfrak{F}(b_0, v_0) = 0$ and $D_v\mathfrak{F}(b_0, v_0)$ is an isomorphism because we are assuming $\sigma[\mathfrak{L}_{(b_0,u_0)}] > 0$. Consequently, the implicit function theorem guarantees the existence, the uniqueness and the regularity of a function v, defined in an ϵ-neighbourhood of b_0, for which $u := v + M$ has the desired properties. The points of this curve are solutions or (1.2) since $v_0 > -M$ and, by continuity, $v(b) > -M$ for all $b \sim b_0$. The fact that the solutions $(b, u(b))$ are linearly asymptotically stable follows easily from $\sigma[\mathfrak{L}_{(b_0,u_0)}] > 0$ and the continuity of the principal eigenvalue with respect to the potential, shortening $\mathscr{U}$ if necessary. Finally, as $(b, u(b))$ solves (1.2), by the theorem of differentiation of Peano, $w := \frac{du}{db}(b)$ satisfies

$$\mathfrak{L}_{(b,u(b))}w(b) = a_+u^p(b) > 0 \quad \text{in } (0,1), \qquad w(0) = w(1) = 0,$$

where a_+ denotes the characteristic function of $(\alpha, 1-\alpha)$. Therefore, the maximum principle implies that $w \gg 0$, which shows the monotonicity of $u(b)$ in b and ends the proof. □

As a byproduct of Proposition 1, the next consequence from Theorem 3.1 holds.

Corollary 1 *Assume $\lambda < 0$. Then there exists $\epsilon > 0$ such that* (1.2) *admits, at least, a linearly asymptotically stable solution for every $b \in [0, \epsilon)$.*

To study the nature of the bifurcation diagrams of (1.2) in a neighbourhood of a neutrally stable positive solution we need the next version of the Picone identity going back to [27, Lemma 4.1].

Lemma 2 *Suppose $\Omega \subset \mathbb{R}^N$, $N \geqslant 1$, is a sufficiently smooth bounded domain of $\mathbb{R}^N$ and let $u, v \in \mathscr{C}^1(\bar{\Omega}) \cap \mathscr{C}^2(\Omega)$ a.e. be such that $v/u \in \mathscr{C}^1(\bar{\Omega})$. Then, for every $f : \mathbb{R} \to \mathbb{R}$ of class $\mathscr{C}^1$,*

$$\int_\Omega f\left(\frac{v}{u}\right)[u\Delta v - v\Delta u] = \int_{\partial\Omega} f\left(\frac{v}{u}\right)\left[u\frac{\partial v}{\partial n} - v\frac{\partial u}{\partial n}\right] - \int_\Omega f'\left(\frac{v}{u}\right)u^2\left|\nabla\frac{v}{u}\right|^2. \tag{4.2}$$

The next result establishes that, around a linearly neutrally stable solution, the bifurcation diagram consists of a subcritical quadratic turning point, filled in by linearly asymptotically stable solutions on its lower half-branch and linearly unstable solutions on the upper one.

Proposition 2 *Let (b_0, u_0) be a linearly neutrally stable positive solution of* (1.2)*, and let $\psi_0 > 0$ be a positive eigenfunction associated with $\sigma[\mathfrak{L}_{(b_0,u_0)}] = 0$. Then there exist $\epsilon > 0$ and a differentiable function $(b, u) : (-\epsilon, \epsilon) \to \mathbb{R} \times \mathscr{C}^1(\bar{\Omega})$ such that $(b(0), u(0)) = (b_0, u_0)$ and $(b(s), u(s))$ is a positive solution of* (1.2) *for each $s \in (-\epsilon, \epsilon)$. Moreover,*

$$u(s) = u_0 + s\psi_0 + w(s), \qquad b(s) = b_0 + b_2s^2 + O(s^3), \tag{4.3}$$

where $w(s) = O(s^2)$ *as* $s \downarrow 0$, $\int_0^1 w(s)\psi_0 = 0$ *for all* $s \in (-\epsilon, \epsilon)$, *and*

$$b_2 = -\frac{p(p-1)}{2} \frac{\int_0^1 a_{b_0} u_0^{p-2} \psi_0^3}{\int_0^1 a_+ u_0^p \psi_0} < 0,$$

where a_+ *denotes the characteristic function of* $(\alpha, 1-\alpha)$. *Furthermore, there is a neighbourhood* $\mathscr{U}$ *of* (b_0, u_0) *in* $\mathbb{R} \times \mathscr{C}^1(\bar{\Omega})$ *such that* $(b, u) = (b(s), u(s))$ *for some* $s \in (-\epsilon, \epsilon)$ *if* $(b, u) \in \mathscr{U}$ *solves* (1.2), *and, as far as the stability of those solutions, we have that*

$$\operatorname{sign} b'(s) = \operatorname{sign} \sigma[\mathfrak{L}_{(b(s),u(s))}] \qquad \textit{for every} \quad s \in (-\epsilon, \epsilon). \tag{4.4}$$

Proof After the usual change of variables $u = v + M$, the existence of ϵ and the functions $b(s)$ and $u(s)$, as well as the local uniqueness and expansions (4.3), follow from [3, Th. 2.1] applied to the operator $\mathfrak{F}$ introduced in (4.1). Indeed, in this case, $D_v\mathfrak{F}(b_0, v_0) = \mathfrak{L}_{(b_0,u_0)}$, where $u_0 = v_0 + M$ is a Fredholm operator of index zero and

$$\ker[D_v\mathfrak{F}(b_0, v_0)] = \operatorname{span}[\psi_0], \qquad \int_0^1 a_+ u_0^p \psi_0 > 0. \tag{4.5}$$

To derive (4.4), which describes the stability of the solutions, we can adapt [4, Prop. 20.8]. Substituting (4.3) in (1.2) and differentiating with respect to s, yields

$$\mathfrak{L}_{(b(s),u(s))} u'(s) = b'(s) a_+ u^p(s) \quad \text{in} \quad (0, 1).$$

Thus, multiplying this equation by a positive eigenfunction associated with $\sigma[\mathfrak{L}_{(b(s),u(s))}]$, say $\psi(s)$, integrating in $(0, 1)$, and integrating by parts, we obtain

$$\sigma[\mathfrak{L}_{(b(s),u(s))}] \int_0^1 u'(s)\psi(s) = b'(s) \int_0^1 a_+ u^p(s)\psi(s),$$

which implies (4.4), as $u'(0) = \psi_0 \gg 0$ implies $u'(s) \gg 0$, $s \sim 0$, by continuity. The formula for b_2 follows by substituting (4.3) in (1.2), differentiating twice with respect to s, particularising at $s = 0$, multiplying by ψ_0 and integrating in $(0, 1)$. To get its sign, recalling (4.5), we should prove that

$$\int_0^1 a_{b_0} u_0^{p-2} \psi_0^3 > 0. \tag{4.6}$$

To show (4.6) we apply Lemma 2 with $v = \psi_0$, $u = u_0$ and $f(t) = t^2$. For this choice, all the boundary terms in (4.2) vanish as $\psi_0(0) = \psi_0(1) = 0$. Moreover,

$$u_0\psi_0'' - \psi_0 u_0'' = -(p-1) a_{b_0} u_0^p \psi_0,$$

and hence the left-hand side of (4.2) becomes $-(p-1)\int_0^1 a_{b_0} u_0^{p-2}\psi_0^3$. Combining this with the fact that the right-hand side of (4.2) equals

$$-2 \int_0^1 \psi_0 u_0 \left| \left(\frac{\psi_0}{u_0} \right)' \right|^2 < 0,$$

https://doi.org/10.1017/S0956792513000429 Published online by Cambridge University Press

because ψ_0 cannot be a multiple of u_0, it is easily seen that (4.6) holds. □

We are ready to complete the proof of Theorem 4.1. First, observe that the arguments in the proof of Theorem 3.1 show the linear stability of (b_0, u_0). Thus, by Propositions 1 and 2, there exists an increasing arc of differentiable curve filled in by linearly asymptotically stable positive solutions of (1.2) in the left neighbourhood, in b, of (b_0, u_0). Let $\mathfrak{C}_0$ denote the lower left-component in b of the set of positive solutions of (1.2) containing the solutions on this left-side arc. As $\mathfrak{C}_0$ consists of solutions of (1.2), it cannot bifurcate from $u = 0$, because $(b, u) \in \mathfrak{C}_0$ implies $u(0) = u(1) = M > 0$. Hence, by construction, and due to Propositions 1 and 2, we have that $(b, u) \in \mathfrak{C}_0$ implies $b \leqslant b_0$ and $u \in (0, u_0]$. Actually $\mathfrak{C}_0$ is a closed arc of differentiable curve. Moreover, one of the following two alternatives occurs:

(A1) Every $(b, u) \in \mathfrak{C}_0$ is linearly asymptotically stable for all $b < b_0$.

(A2) There exists a neutrally stable positive solution $(b_1, u_1) \in \mathfrak{C}_0$ with $b_1 < b_0$.

Alternative (A2) is excluded as due to Proposition 2 there should not exist any positive solution on the right-side neighbourhood of (b_1, u_1), which contradicts the construction of $\mathfrak{C}_0$ by the left-path-following from (b_0, u_0). Therefore, alternative (A1) occurs, and hence $\mathfrak{C}_0$ consists of linearly asymptotically stable solutions, except, possibly, (b_0, u_0). By the implicit function theorem (see the proof of Proposition 1), this entails $(0, \theta_{[\lambda,M]}) \in \mathfrak{C}_0$, where $\theta_{[\lambda,M]}$ is the one defined in Section 1. Also, by the local uniqueness given by Propositions 1 and 2, and compactness, the solutions along $\mathfrak{C}_0$ are the unique ones close to $\mathfrak{C}_0$. Suppose that $(b_0, \tilde{u}_0)$ is a linearly stable solution with $\tilde{u}_0 \neq u_0$. Reasoning as above, there exists another component of the set of positive solutions of (1.2), denoted by $\tilde{\mathfrak{C}}_0$, such that $(0, \theta_{[\lambda,0]}) \in \tilde{\mathfrak{C}}_0$. Consequently, $\mathfrak{C}_0 = \tilde{\mathfrak{C}}_0$ and therefore, since $\mathfrak{C}_0$ is a differentiable curve, $\tilde{u}_0 = u_0$, which is a contradiction.

Corollary 2 *Suppose* (b_0, u_0) *is a linearly neutrally stable solution of* (1.2). *Then* (1.2) *cannot admit any positive solution for* $b > b_0$.

Proof By [30, Th. 3.5], $b_0 > 0$. Moreover, by Proposition 2, the set of positive solutions of (1.2) in the neighbourhood of (b_0, u_0) is a subcritical quadratic turning point. Suppose (1.2) admits a solution (b_1, u_1) with $b_1 > b_0$. Then, due to Theorem 3.1, there exists a positive solution $(b_1, u_{\min})$, which is linearly stable. Adapting the proof of Theorem 4.1, there exists a differentiable curve $\mathfrak{C}_0$ such that $(b_1, u_{\min}) \in \mathfrak{C}_0$, which is filled in by linearly asymptotically stable solutions of (1.2), except, at most, $(b_1, u_{\min})$. By Theorem 4.1, $(b_0, u_0) \in \mathfrak{C}_0$, which is impossible. □

5 Conclusions

In this paper we computed the (rather intricate) bifurcation diagrams of (1.2) by coupling a pseudo-spectral method with collocation with a path-following solver designed by the authors for this work. The numerics suggested the following features:

(a) For every $\lambda < 0$, there is $b_c = b_c(\lambda) > 0$ such that the interval $(-\infty, b_c(\lambda)]$ provides us with the set of b's for which (1.2) admits a positive solution.

https://doi.org/10.1017/S0956792513000429 Published online by Cambridge University Press

(b) $\lim_{\lambda \downarrow -\infty} b_c(\lambda) = +\infty$.

(c) The unique stable positive steady state of (1.1) is the minimal one, although (1.2) can admit an arbitrarily large number of equilibria.

Properties (a) and (b) are proved in Section 3, and property (c) is proved in Section 4.

Regarding (1.1) as a model for the evolution of a species u in an unfavourable environment, where the individuals compete for the available resources in some regions while they cooperate in others, our analysis shows how the dynamics becomes more and more complex as the toxicity of the environment blows up, quantifying such complexity through the computation of the degree of instability of all the steady states. This astonishing result, rather unexpected, suggests the development of empirical studies to validate our predictions. Plant interactions in arid regions might be easily reproduced in laboratory and should give more insight into this problem. As a consequence of the multiplicity of the steady states and the dimensions of their unstable manifolds, under the appropriate initial conditions, the species might approximate any of them by taking the initial values on their stable manifolds. Otherwise, if the initial values lie outside the stable manifolds of the steady states, the solution might oscillate for some time among some of the steady states of the problem and then either blow up as an effect of facilitation, or approximate the minimal equilibrium of the problem, which is a unique local attractor.

Acknowledgements

This research has been supported by Projects MTM2009-08259 and MTM2012-30669, and Grant BES-2010-039030 of the Spanish Ministry of Economy and Competitiveness.

References

[1] Alama, S. & Tarantello, G. (1996) Elliptic problems with nonlinearities indefinite in sign. *J. Funct. Anal.* **141**, 159–215.

[2] Allgower, E. L. & Georg, K. (2003) *Introduction to Numerical Continuation Methods*, SIAM Classics in Applied Mathematics 45, SIAM, Philadelphia, PA.

[3] Amann, H. (1974) Multiple positive fixed points of asymptotically linear maps. *J. Funct. Anal.* **17**, 174–213.

[4] Amann, H. (1976) Fixed point equations and nonlinear eigenvalue problems in ordered Banach spaces. *SIAM Rev.* **18**, 620–709.

[5] Amann, H. & López-Gómez, J. (1998) A priori bounds and multiple solutions for superlinear indefinite elliptic problems. *J. Diff. Equ.* **146**, 336–374.

[6] Berestycki, H., Capuzzo-Dolcetta, I. & Nirenberg, L. (1994) Superlinear indefinite elliptic problems and nonlinear Liouville theorems. *Top. Meth. Nonl. Anal.* **4**, 59–78.

[7] Berestycki, H., Capuzzo-Dolcetta, I. & Nirenberg, L. (1995) Variational methods for indefinite superlinear homogeneous elliptic problems. *Nonl. Diff. Equ. Appns.* **2**, 553–572.

[8] Bertness, M. D. & Callaway, R. M. (1994) Positive interactions in communities. *Trends Ecol. Evol.* **9**, 191–193.

[9] Brezzi, F., Rappaz, J. & Raviart, P. A. (1980) Finite dimensional approximation of nonlinear problems, part I: Branches of nonsingular solutions. *Numer. Math.* **36**, 1–25.

[10] Brezzi, F., Rappaz, J. & Raviart, P. A. (1981) Finite dimensional approximation of nonlinear problems, part II: Limit points. *Numer. Math.* **37**, 1–28.

[11] Brezzi, F., Rappaz, J. & Raviart, P. A. (1981) Finite dimensional approximation of nonlinear problems, part III: Simple bifurcation points. *Numer. Math.* **38**, 1–30.

[12] Callaway, R. M. & Walker, L. R. (1997) Competition and facilitation: A synthetic approach to interactions in plant communities. *Ecology* **78**, 1958–1965.

[13] Canuto, C., Hussaini, M. Y., Quarteroni, A. & Zang, T. A. (1988) *Spectral Methods in Fluid Mechanics*, Springer, Berlin, Germany.

[14] Connell, J. H. (1983) On the prevalence and relative importance of interspecific competition: Evidence from field experiments. *Amer. Natur.* **122**, 661–696.

[15] Crouzeix, M. & Rappaz, J. (1990) *On Numerical Approximation in Bifurcation Theory*, Recherches en Mathématiques Appliquées 13. Masson, Paris, France.

[16] Doedel, E. J. & Oldeman, B. E. (2012) AUTO-07P: Continuation and bifurcation software for ordinary differential equations [online]. Available at: http://www.dam.brown.edu/people/sandsted/auto/auto07p.pdf. Accessed on 7 October 2013.

[17] Eilbeck, J. C. (1986) The pseudo-spectral method and path-following in reaction–diffusion bifurcation studies. *SIAM J. Sci. Stat. Comput.* **7**, 599–610.

[18] García-Melián, J. (2011) Multiplicity of positive solutions to boundary blow up elliptic problems with sign-changing weights. *J. Funct. Anal.* **261**, 1775–1798.

[19] Gilbarg, D. & Trudinger, N. S. (2001) *Elliptic Partial Differential Equations of Second Order*, Classics in Mathematics, Springer, Berlin, Germany.

[20] Golubitsky, M. & Shaeffer, D. G. (1985) *Singularity and Groups in Bifurcation Theory*, Springer, Berlin, Germany.

[21] Gómez-Reñasco, R. & López-Gómez, J. (2000) The effect of varying coefficients on the dynamics of a class of superlinear indefinite reaction diffusion equations. *J. Diff. Equ.* **167**, 36–72.

[22] Gómez-Reñasco, R. & López-Gómez, J. (2001) The uniqueness of the stable positive solution for a class of superlinear indefinite reaction diffusion equations. *Diff. Int. Equ.* **14**, 751–768.

[23] Gómez-Reñasco, R. & López-Gómez, J. (2002) On the existence and numerical computation of classical and non-classical solutions for a family of elliptic boundary value problems. *Nonlinear Anal. Theory Methods Appl.* **48**, 567–605.

[24] Hutchinson, G. E. (1965) *The Ecological Theater and the Evolutionary Play*, Yale University Press, New Haven, CT.

[25] Keller, H. B. (1986) *Lectures on Numerical Methods in Bifurcation Problems*, Tata Insitute of Fundamental Research, Springer, Berlin, Germany.

[26] López-Gómez, J. (1988) *Estabilidad y Bifurcación Estática. Aplicaciones y Métodos Numéricos*, Cuadernos de Matemática y Mecánica, Serie Cursos y Seminarios N° 4, Santa Fe.

[27] López-Gómez, J. (1997) On the existence of positive solutions for some indefinite superlinear elliptic problems. *Comm. Part. Diff. Equ.* **22**, 1787–1804.

[28] López-Gómez, J. (1999) Varying bifurcation diagrams of positive solutions for a class of indefinite superlinear boundary value problems. *Trans. Amer. Math. Soc.* **352**, 1825–1858.

[29] López-Gómez, J. (2005) Global existence versus blow-up in superlinear indefinite parabolic problems. *Sci. Math. Jpn.* **61**, 493–516.

[30] López-Gómez, J. (2005) Metasolutions: Malthus versus Verhulst in population dynamics. A dream of Volterra. In: M. Chipot & P. Quittner (editors), *Handbook of Differential Equations 'Stationary Partial Differential Equations'*, Elsevier Science, B. V. North Holland, Amsterdam, Netherlanda, Chapter 4, pp. 211–309.

[31] López-Gómez, J., Eilbeck, J. C., Duncan, K. & Molina-Meyer, M. (1992) Structure of solution manifolds in a strongly coupled elliptic system, IMA Conference on Dynamics of Numerics and Numerics of Dynamics (Bristol, 1990). *IMA J. Numer. Anal.* **12**, 405–428.

[32] López-Gómez, J. & Molina-Meyer, M. (1994) The maximum principle for cooperative weakly coupled elliptic systems and some applications. *Diff. Int. Equ.* **7**, 383–398.

[33] López-Gómez, J. & Molina-Meyer, M. (2006) Superlinear indefinite systems: Beyond Lotka–Volterra models. *J. Differ. Equ.* **221**, 343–411.

[34] López-Gómez, J. & Molina-Meyer, M. (2006) The competitive exclusion principle versus biodiversity through segregation and further adaptation to spatial heterogeneities. *Theor. Popul. Biol.* **69**, 94–109.

[35] López-Gómez, J. & Molina-Meyer, M. (2007) Biodiversity through co-opetition. *Discrete Contin. Dyn. Syst. B* **8**, 187–205.

[36] López-Gómez, J. & Molina-Meyer, M. (2007) Modeling coopetition. *Math. Comput. Simul.* **76**, 132–140.

[37] López-Gómez, J., Molina, M. & Villareal, M. (1992) Numerical coexistence of coexistence states. *SIAM J. Numer. Anal.* **29**, 1074–1092.

[38] López-Gómez, J., Tellini, A. & Zanolin, F. (2014) High multiplicity and complexity of the bifurcation diagrams of large solutions for a class of superlinear indefinite problems. *Comm. Pure Appl. Anal.* **13**(1), 1–73.

[39] Mawhin, J., Papini, D. & Zanolin, F. (2003) Boundary blow-up for differential equations with indefinite weight. *J. Diff. Equ.* **188**, 33–51.

[40] Pugnaire, F. I. (Editor) (2010) *Positive Plant Interactions and Community Dynamics*, Fundación BBVA, CRC Press, Boca Raton, FL.

[41] Saffo, M. B. (1992) Invertebrates in endosymbiotic associations. *Amer. Zool.* **32**, 557–565.

[42] Shoener, T. W. (1983) Field experiments on interspecific competition. *Amer. Natur.* **122**, 240–285.

[43] Wulff, J. L. (1985) Clonal organisms and the evolution of mutualism. In: J. B. C. Jackson, L. W. Buss & R. E. Cook (editors), *Population Biology and Evolution of Clonal Organisms*, Yale University Press, New Haven, CT, pp. 437–466.